Fall 11-15-2021

Cognizant Composites: Seamless Integration of Circuitry and Sensors into Structural Composites

Reuben Fresquez
University of New Mexico

Reuben Fresquez

Candidate

Computer Science

Department

This thesis is approved, and it is acceptable in quality and form for publication:

Approved by the Thesis Committee:

Leah Buechley , Chairperson

Mahmoud Reda Taha

Gruia-Catalin Roman

COGNIZANT COMPOSITES:
SEAMLESS INTEGRATION OF CIRCUITRYAND SENSORS INTO STRUCTURAL COMPOSITES

by

REUBEN FRESQUEZ

PREVIOUS DEGREES
B.S., COMPUTER SCIENCE, UNIVERSITY OF NEW MEXICO, 2020

THESIS

Submitted in Partial Fulfillment of the
Requirements for the Degree of

Masters of Science
Computer Science

The University of New Mexico
Albuquerque, New Mexico

December, 2021

COGNIZANT COMPOSITES:

SEAMLESS INTEGRATION OF CIRCUITRY AND SENSORS INTO STRUCTURAL COMPOSITES

by

Reuben Fresquez

M.S., Computer Science, University of New Mexico, 2021

B.S., Computer Science, University of New Mexico, 2020

ABSTRACT

This thesis describes a set of novel techniques for embedding sensors, circuitry, and electronics into structural composites. I leverage recent developments in human computer interaction to create sensors and circuitry that are seamlessly incorporated into structural composites. I fabricate bend and compression sensors, along with circuitry, from textiles, which enables me to add electronic capabilities without impacting the composite's structural integrity. I describe the construction of these "cognizant composites" and demonstrate their functionality. I also explore techniques for embedding standard electronic components, including microcontrollers, into structural composites. Potential applications of this technology include buildings that can warn occupants if load-bearing components

are experiencing unexpected strain, bridges that can document traffic patterns, and delicate structures, like satellites, that can detect and perhaps control their own shape.

TABLE OF CONTENTS

1 PREFACE

The research in this thesis is part of a collaborative effort between The University of New Mexico's Department of Computer Science and Department of Civil Engineering to research and develop cognizant composites. I along with Mohammed Jaradat developed and tested all the samples used in this thesis. My work focused on sensor development and circuitry integration, and his focused on material selection and composite construction. Together we combined our work to create these cognizant composites and performed structural tests that are standard in Civil Engineering.

2 INTRODUCTION

Much of our physical infrastructure is built from structural composites (SCs)— materials consisting of a polymer matrix reinforced with layers of high strength fibers. Buildings, bridges, vehicles, and spacecraft include SCs, and, in the future, HSCs can be expected to be deployed in an increasing number of contexts, as they emerge as a stronger, lighter, and greener replacement for cement-based materials.

Structural health monitoring, the ability to keep track of the structural integrity of a building material over time, is an important topic in composites research communities [7]. The safety of our infrastructure would be dramatically improved if we were able to collect information about changes in a material's strength over time. We might be able to, for instance, predict and prevent incidents like the recent collapse of an apartment complex in Miami, Florida [32].

This thesis explores how to create composites that perform both as structural elements and as sensors. These "cognizant composites" can monitor and potentially react to their own internal states. They can detect the strains and stresses they are subject to and, through embedded computational elements, may be able to sound alerts about changes in structural health or perhaps even take corrective action when necessary. They may also be integrated into larger systems aimed at monitoring structural health.

3 PREVIOUS WORK

A significant amount of previous work has involved embedding sensors into different material substrates, both in the civil engineering and Human Computer Interaction (HCI) communities. In composite research communities, this previous work can be sorted into two broad categories: embedded existing sensors into composite materials and creating sensors from composite materials.

In the first category, for instance, accelerometers [24] and piezoelectric wafer transducers [34] placed on the outside surface of composites have been used to monitor and evaluate the damage induced during mechanical testing. The utility of sensors that are placed on the surface of composites are limited. For many applications, it is much more valuable to be able to monitor their interior state. Some researchers have embedded off-the-shelf sensors inside of composites. Sensors have included piezoelectric sensors [2,37], capacitive sensors, and temperature sensors [38]. Fiber optic bend sensors have been used as strain sensors in different contexts [15,26]. Embedded off-the-shelf sensors provide a range of useful sensing capabilities, but have a disruptive impact on the performance of composites [6].

To address these limitations, another body of research has explored turning the composite material itself into a sensor. A range of work has explored functionalizing polymer resins by mixing them with metal and carbon powers, and carbon nanotubes [1,9,17,23]. When the resin is the sensing material, the entire composite functions as a large homogeneous sensor, which may or may not be desirable. Carbon fiber can serve as both a structural and electrical element in

composites, and through careful placement can facilitate the design of more targeted sensing capabilities. For example, it has been used to detect composite cracking [12] and compression [36].

In research that comes closest to the work described here, Boehle et al. and Sebastian et al. developed and refined a technique to grow “fuzzy fiber sensors”, by applying carbon nanotubes to glass fibers, which were then used to measure strain [3,31]. Similarly, Krushnamurty et al. propose a technique to use in-situ polymerization to add conductive polymers to resin used to build composites, and Macasaquit et al. detail a process for the optimization of conductive composite textiles through in-situ polymerization [19,22]. Composite-based approaches have the advantage of not interfering with composite integrity. A significant drawback, however, remains that circuitry and other electronics still have to be located outside of the composite. For instance, to collect strain measurements, Sebastian et al. glued wires to their fuzzy sensors with conductive epoxy [31].

Structural composites are fiber reinforced, making smart textiles and fabric sensors an important body of related research. Significant work in the HCI community is focused on the realm of flexible circuitry to expand the usability of sensing technology. Smart textiles can be incorporated into clothing to incorporate unobtrusive sensing and processing into wearable garments. For example, Enokibori et al. are able to estimate joint angles using textile sensors in elbow supports and sweaters [10] and Glauser et al. are able to estimate hand poses using a stretch sensing gloves and machine learning [13]. Similarly, Schneegass et al. explore some of the different applications of smart textiles and how to develop

technologies that are independent of the fabric to allow for rapid prototyping [30], and Klamka et al. propose a tool for iron-on smart textiles that allows for rapid prototyping through a handheld dispenser tool that directly applies continuous functional tapes that can be configured to create complex circuits [16].

Another related body of research in HCI is focused on embedding sensors in cast structures. Several researchers have explored using liquid metal in silicone channels to create stretchable circuits and sensors. For example, Nagels et al. utilizes liquid metal within silicone channels to construct multi-layer flexible circuitry creating touch, proximity, sliding, pressure, and strain sensors [27]. Using a similar approach Kramer et al. use conductive channels of liquid metal in silicone to create a pressure sensitive keypad [18]. Additional work has been done in layering electronics in cast structures. Slyper et al. layer electronics between silicone pours in order to create sensors that detect deformations in the cast structure [33]. Boem et al. conducted an extensive survey of 131 papers regarding Deformable interfaces to be used as an overview of existing non-rigid interfaces, and their applications [4].

My work is unique in a few ways. I introduce a new method for creating sensors and circuitry that are a seamless element of the composite structure and do not negatively impact its performance. The fact that I can combine sensing materials with circuit structures allows me to create complex electronic configurations within composites. Through mechanical and electrical testing, I demonstrate that the materials and techniques developed can be deployed in civil engineering and HCI contexts.

4 PRELIMINARY PROTOTYPE

I began my work by prototyping a smart composite with a sensor and flexible circuitry to demonstrate the ability to embed circuitry and electronics into structural composites. The process used to construct the composite is the same as that described in Section 4, with a two-part polyurethane resin as the matrix and fiberglass as a reinforcement textile. The sensor was constructed by layering 3 strips of Velostat between two copper fabric electrodes. Velostat is a 0.1016mm thick, carbon impregnated black polyethylene film with a resistance of < 500 Ohms/cm [21]. Velostat is a piezoresistive material whose electrical resistivity changes when mechanical strain is applied. When sandwiched between the copper electrodes, the change in resistance can be measured and used as an indication of strain being applied [29]. The design enables me to monitor transverse resistance (the resistance through the material in the z direction) across the length of the sensor, ensuring that the measurement is not localized to a specific area of the sensor.

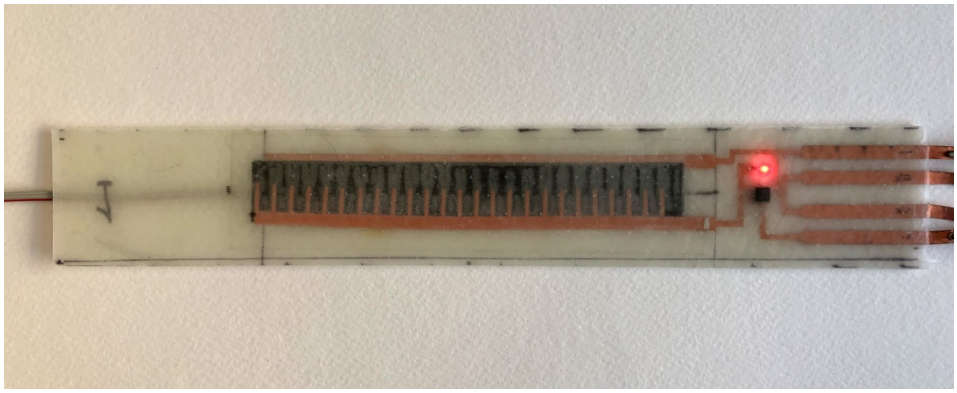

Figure 1: Preliminary prototype sample.

The circuit is constructed using a copper plated polyester taffeta from LessEMF that has a thickness of .08mm, a weight of 80 g/m2, and a surface resistivity of 0.05 Ohms/square [21]. The circuit construction process is detailed in Section 5.3. Once the textile circuit is assembled an ATtiny84 microcontroller, a resistor, and an LED are soldered to the circuit. The microcontroller takes reading from the Velostat sensor and transmits the resistance readings using serial communication. As the change in resistance increases, the brightness of the LED increases.

The samples were then tested using the three-point bending test described in more detail in Section 6.3 to detect bending strain. The test is performed by applying an intermediate load to a specimen spanning two supports. Figure 2 shows plots of the resistance values I recorded from the sensors plotted versus strain measurements recorded from an external strain gauge. Figure 2, left shows the sensor data and Figure 2, right shows the percentage change in resistance versus strain. As can be observed in these graphs, for each individual sensor there seems to be a clear correlation between the change in resistance, as measured by the sensors, and the change in strain.

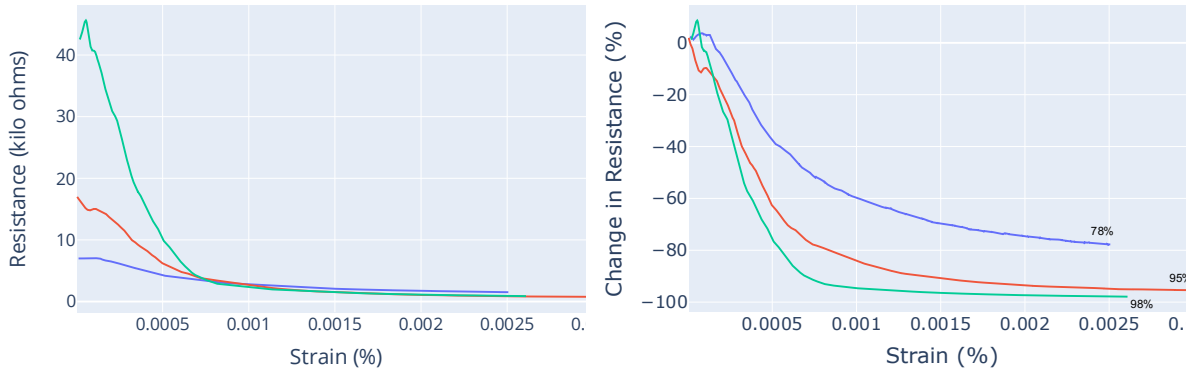

Figure 2: Three-point bend test, embedded sensor measurements. Left: Resistance vs. strain. Right: % change in resistance vs. strain.

These results were promising. We were able to demonstrate the ability to fabricate composite plates with embedded electronics that sense strain. However, because Velostat is a plastic, the structural integrity of the composites was compromised. The sensors were not fully integrated into the composite. The composite layers surrounding the sensors could not bond to the Velostat, resulting in delamination and air pockets formed around the sensors as can be seen in Figure 1.

I hypothesize that this delamination is at least partly responsible for the noise present in the collected data as well as the variation in the slope of the resistance vs. strain curves calculated for each sensor. Similarly, polyurethane resin has a high elasticity resulting in the composite experiencing a small percentage of strain over the course of the test. As can be seen in Figure 2, the percentage change in resistance experienced by the sensors ranged from 78% (at 0.0025% strain) to 98% (at 0.0026% strain), with the median sensor experiencing a 95% change (at

0.003% strain). It is also of value to note that the resistance decreases quite quickly, and the resistance for all three samples converges and approaches zero after experiencing very little strain (around 0.001% strain).

This preliminary prototype demonstrates the ability to embed circuits and electronics in a structural composite, but before the sensors can be used to predict strain reliably, I needed to develop a sensor that can be seamlessly integrated into the composite. This process is detailed in the following sections where I introduce a new method for creating sensors and circuitry that are a seamless element of the composite structure and do not negatively impact its performance.

5 SEAMLESS INTEGRATION OF SENSORS

Once I was able to demonstrate the ability to embed circuitry and electronics in a structural composite, I needed to develop a sensor material that is a seamless element of the composite. In this section, I detail a new method for creating sensors and circuitry that are seamless elements of the composite structure.

These new composites are constructed using a fiberglass reinforcement textile and vinyl ester resin. Each composite is composed of 15 layers of fiberglass fabric that are saturated with resin. Circuitry and sensors are embedded in one of these layers. Each part of the construction process is described in detail below.

5.1 Composite Materials

My Civil Engineering colleagues chose a plain weave fiberglass fabric as a reinforcement material because it provides stiffness and strength without interfering

with electrical functionality. Carbon fiber, another common reinforcement material, was avoided since it is electrically conductive. We used an E-glass fabric, a light-weight woven fiberglass, with an average weight of 123 g/m2 and fabric thickness of 0.15mm supplied by US Composites [35]. The failure strength of the two fiber directions is 7 and 6 N/mm2 respectively.

We used a Hydrex® 100 33350 vinyl ester resin from US Composites [35], which is pre-promoted to cure at room temperature with methyl ethyl ketone peroxide (MEKP) as a catalyst. We used a mix ratio of catalyst to resin of 1.25% of the resin weight. This resin has a relatively low viscosity of 500 cps which helps in the fiber impregnation and a gel time of 35-40 minutes. The tensile strength, modulus, and strain to failure are 83 MPa, 3.5 GPa, and 4%, respectively. Vinyl ester resin is much stiffer than polyurethane resin, making it so that the new composite samples experience much more strain during testing compared to the preliminary prototype samples.

5.2 Sensor Material

I employ a technique described by Honnet et al. to create a piezoresistive textile that forms the basis of the sensors [14]. Piezoresistive materials experience the piezoresistive effect. The piezoresistive effect is a change in electrical resistance when strain is applied. An in-situ polymerization process is employed to coat a textile substrate with a carbon-based piezoresistive material. The resulting textile has an electrical resistance that changes predictably in response to strain. I adjusted Honnet et al.'s polymerization recipe to apply the technique to fiberglass.

This enables us to endow the foundational composite material with the desired electrical properties. The benefit of in-situ polymerization is that the textile's mechanical properties are preserved as polymerization happens around and within each thread. This enables seamless sensor integration in the composite by reducing the chances of improper impregnation by the resin which leads to debonding. It also significantly avoids creating internal stresses that are due to stiffness incompatibility between the composite layers which can also lead to debonding and premature failure of the composite.

Polymerization occurs when a monomer (pyrrole) is exposed to an oxidizing agent (iron chloride). Oxidization breaks atomic bonds in the monomer allowing for polymer chains (polypyrrole) to form. Synthesized polypyrrole has a core of carbon chains making it conductive. In the presence of fiber glass, the polypyrrole polymers form around and within each strand of fiber. The process of polymerization that I used is described briefly below. More detailed information can be found in [14]. I used pyrrole and iron(III) chloride hexahydrate from Fischer Scientific [11].

To polymerize a sheet of fiberglass, I first measure out an amount of water appropriate for the fiberglass to ensure that the fiberglass can sit comfortably in the water without clumping. I then add Pyrrole to the water, creating a water pyrrole solution with the previously measured water, using a ratio of 1000:25 water to pyrrole—25ml of pyrrole for every 1 liter of water. The fiberglass is then soaked in the water pyrrole solution for approximately 10-15 minutes. The mixture is stirred continuously during this period.

Next, I prepare the iron chloride. I use a 1:10, water to iron chloride ratio—10g of iron chloride for every 1 liter of water. The iron chloride is ground into a fine powder using a mortar and pestle and then diluted with a small amount of water to ensure dispersion. This slurry is added to the water pyrrole solution. The entire mixture is then agitated for approximately 30 minutes to achieve polymerization of the fiberglass. As the polymers begin to form, the fiberglass and the mixture begins to darken. The process is complete once the fiberglass has turned black. At this point, it can be removed from the mixture, rinsed in cold water, and air-dried. Figure 3 shows images of this process.

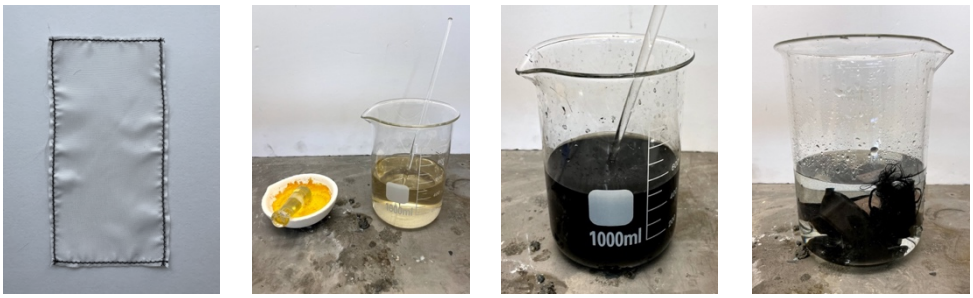

Figure 3: The polymerization process. From left to right: a piece of fiberglass with sewn edges to prevent fraying, the water-pyrrole and iron chloride chemicals, polymerization taking place, polymerized materials being rinsed in water.

Due to the stiffness and weave of the fiberglass, the edges tend to fray rapidly. I found that without reinforcement around the edge of the fiberglass sheet, the fabric would come apart during the polymerization process. I tried three different edge reinforcements, laser cutting, taping, and sewing. Laser cutting the fiberglass seals the edges with heat, but vigorous stirring still manages to unravel the edges, as is shown in Figure 4, left. Taping the edges prevents fraying but

makes the sheet too stiff to stir thoroughly and can result in uneven polymerization. Sewing the edges prevents fraying while maintaining flexibility. After the fiberglass sheet is functionalized, I cut it with a laser cutter into pieces that can be used for testing and constructing sensors.

The conductivity of the final sample depends on the amount of chemicals added to the water. I found that fiberglass was more difficult to polymerize than other textiles; it took a more concentrated chemical mix to polymerize fiberglass compared to other materials. The difficulty in polymerizing the fiberglass fabric may be attributed to the chemical coating that keeps the fiberglass filaments from abrading and breaking. In the process described by Honnet et al., they note that increasing the amount of iron chloride relative to amount of pyrrole increases the conductivity of the polymerized material [14]. I tested a range of ratios of iron chloride to pyrrole to functionalize the fiberglass, including 10mg, 5g, and 10g per 25ml of pyrrole and one liter of water.

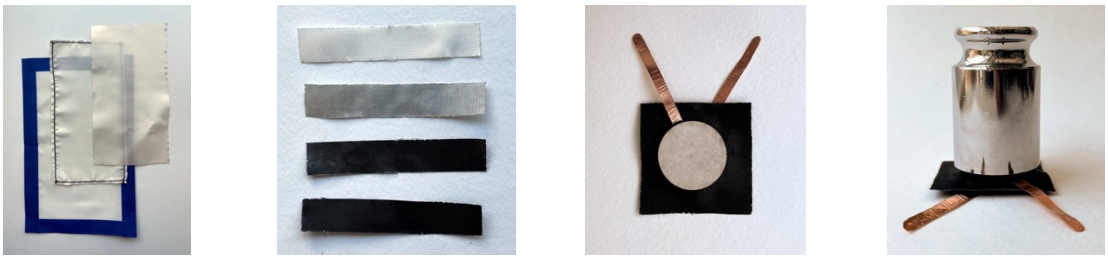

Figure 4: From left to right: different ways of sealing fiberglass edges; polymerized fiberglass made with different recipes (top to bottom): plain fiberglass, 10mg, 5g, and 10g of iron chloride per 25ml of pyrrole; transverse resistance test.

Samples of the three different iron chloride to pyrrole ratios were tested to compare resistance and functionality. 5 x 5 cm samples were created following the three recipes described above. I then measured the transverse resistance (the resistance through the material in the z direction) of the samples by sandwiching them between two rigid copper electrodes, each with a diameter of 2cm. Weights were placed on top of the samples to measure their response to compression, Figure 4, right. The results of this set of tests, which is modeled after a similar one conducted by Honnet et al. [14], can be seen in Table 1. The conductivity of the samples increased with the amount of iron chloride. 10mg resulted in a textile that had no useful electrical properties. Both the 5g and 10g recipes produce functional piezoresistive fiberglass.

Table 1: Transverse resistance for different amounts of iron chloride and weight.

Iron Chloride	Resistance (kΩ), 50 g weight	Resistance (kΩ), 500 g weight	Resistance (kΩ), 1000 g weight
10mg	---	---	---
5g	35.50	11.73	6.51
10g	7.66	4.60	2.65

While testing the three iron chloride to pyrrole ratios for polymerizing the fiberglass fabric, I was looking for an even coating of polymers on the surface of the fiberglass and a sufficiently wide range of resistance reading in response to compression. While the 5g sample produced a wide range of resistance reading as

reported in Table 1, it had uneven polymerization resulting in a patchy surface. 5g was enough to functionalize the fiberglass, but I was able to obtain more consistent polymerization with 10g of iron chloride. The 10g recipe produced suitable polymerization and was used for the sensors fabricated and tested in the remainder of Section 5 and Section 6.

5.3 Circuitry and Sensor Integration

Once I have a sensing material, I can use it to build a range of sensing structures by adding textile circuitry. This circuitry is constructed from conductive fabric using the technique described by Buechley and Eisenberg in [5]. Conductive fabric is laser-cut and then applied to a backing fabric, in my case fiberglass, with a heat-activated adhesive. The resulting “textile circuit board” is soft and flexible. It is also porous, which enables resin to saturate the circuit during the composite fabrication process. I used a copper plated polyester taffeta from LessEMF that has a thickness of .08mm, a weight of 80 g/m2, and a surface resistivity of 0.05 Ohms/square [21]. Heat-n-bond iron-on adhesive was used to attach this fabric to fiberglass. Figure 5 shows images that detail the process of a textile circuit board construction that includes one of the sensors along with an ATtiny84 microcontroller, a resistor, and an LED.

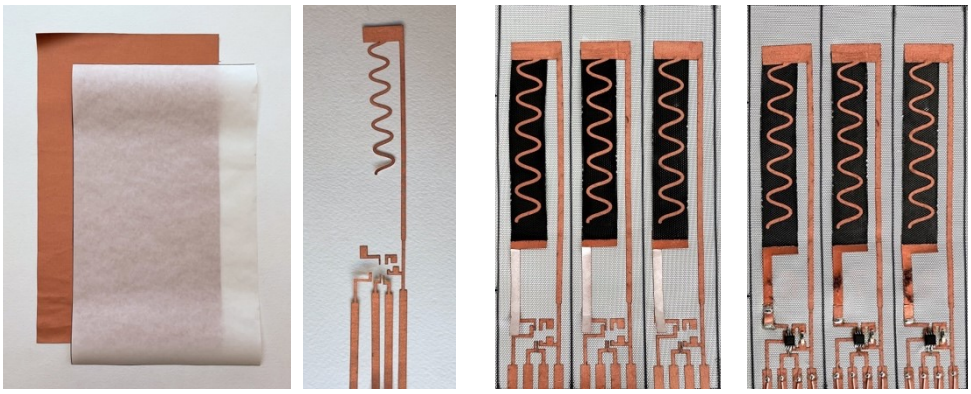

Figure 5: The sensor and circuit construction process. From left to right: adhesive is applied to copper fabric, which is then laser-cut and attached to a larger fiberglass sheet. Finally, components are soldered to the circuit.

I tested a few different sensor configurations before settling on the design seen in Figure 5, where two strips of zig-zagging copper fabric are attached to the bottom and top of a strip of polymerized fiberglass. This design enables us to monitor transverse resistance across the length of the sensor, ensuring that the measurement is not localized to a specific area of the sensor. One end of the sensor is attached to the ADC of a microcontroller in parallel with a pullup resistor and the other end is attached to ground. The pull up resistor allows current to flow from power to the ADC input pin of the micro controller. While the sensor is connected to the ADC input pin, current is directed through sensor to ground, and the ADC input pin will then read the sensors resistance. As the resistance of the sensor changes with strain, the pin will read that change in resistance.

5.4 Composite Fabrication Process

My sensors were placed on the third layer from the bottom of a 15-layer composite. The composite “plates” (samples) produced in this work were fabricated

using a vacuum-assisted “hand layup” process in which layers of fiberglass are saturated with resin, stacked on top of each other, and then placed in a vacuum bag in order to remove air bubbles and voids [20]. All composite plates were left under vacuum at room temperature for 24 hours at a vacuum pressure of 2.3 x 10-2 Torr. The plates were then placed in an oven for 8 hours at 80 °C for post curing. Figure 6 shows the hand layup fabrication setup and a plate during fabrication.

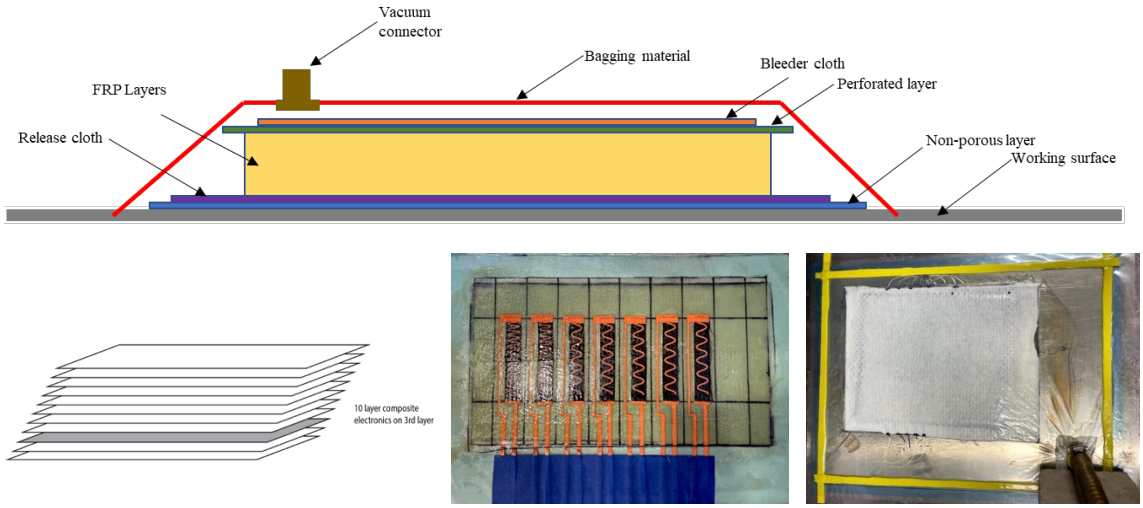

Figure 6: The composite construction process. Top: hand layup diagram. Bottom, from left to right: composite diagram, a composite with sensors during construction, a vacuum eliminating air while composite is curing.

Several individual test specimens were produced from each plate. The plate shown in Figure 6, for example, produced seven different test specimens, each containing a single sensor. The specimens were cut with a water-jet cutter to avoid damaging the composite by cutting it with saws. We created specimens for two different tests, which are described in detail below.

6 COMPOSITE TESTING

6.1 Structural Integrity

To investigate how the sensors and circuitry impact the structural integrity of the composites, we conducted a tension test, in which the composite plate is subjected to a uniaxial tension load until failure. The selection of tension test to represent integrity is attributed to the fact that fiber reinforced polymer composites are typically used to resist tension loads.

Figure 7: Left: Uniaxial tension test. Right: samples with sensor (top) and without (bottom).

We constructed five samples without sensors and five with sensors for this integrity test. The samples are shown in Figure 7, right. Each sample is approximately 250mm long, 21mm wide, and 2.7mm thick. There is slight variation in the exact size of individual samples due to variability in waterjet cutting and the fact that the sensors introduce a slight variation in height in the middle of the sensor samples.

Tests were conducted using a Bionix serohydraulic universal testing machine that has a load cell capacity of 25 kN (±1 N) and a maximum stroke of 130 mm (±1 mm). The top and bottom of the sample are attached to a testing machine using mechanical wedge anchors. A displacement control test was used with a displacement rate of 2 millimeters per minute, see Figure 7. The force exerted by the machine during testing is recorded. Additionally, strain (the normalized sample elongation) is measured using an axial extensometer attached to the specimen with a gauge length of 25.4 mm and a strain range of +50% and -20%. The machine pulled the sample apart at a rate of 2mm/minute. Strain and force data was collected through a FlexStar MTS® 793 data acquisition system with a sampling rate of 1Hz. These measurements enable us to determine the tensile failure strength and the corresponding failure strain of the composite material. Other critical mechanical characteristics such as the elastic modulus can also be determined.

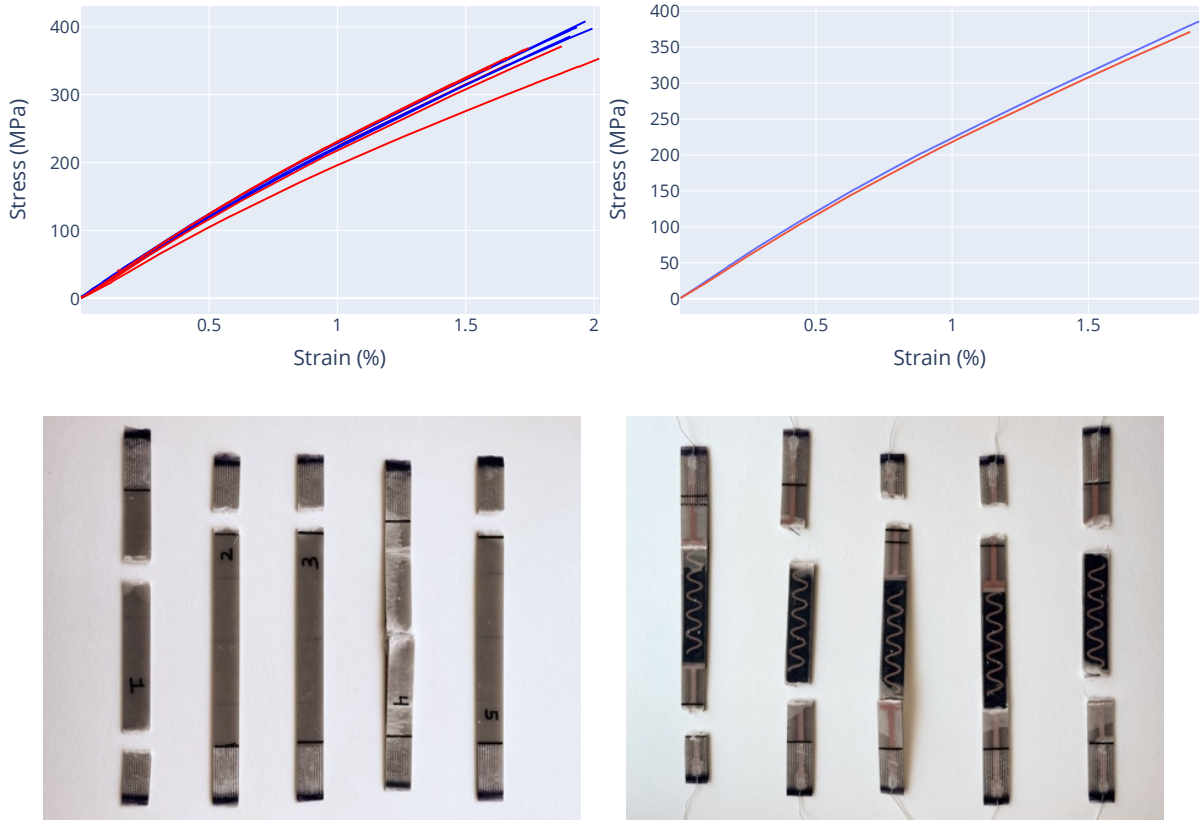

Figure 8: Top: Stress vs strain curves for samples with sensors (red) and without (blue). Bottom: Broken samples, without sensors (left) and with (right).

Figure 8 shows plots of stress vs. strain along with images of samples after testing. The curves for samples without sensors are shown in blue and with sensors are shown in red. As can be observed in Figure 8, there is essentially no difference in strength between the two conditions. The top right of Figure 8 shows plots for the median samples in each category. It is worth noting that there are different breaking patterns between the two sets of samples. As seen in the bottom of Figure 8, the samples with sensors broke consistently on either side of the sensor, where

the samples without sensors broke closer to the mechanical grip. This can possibly be attributed to the extra layer of fiberglass the sensor adds to the composite.

A two-tailed test was performed on the stress and strain data for both the specimens with and without sensors to evaluate the impact embedding the sensors has on the reliability of the composite. A two-tailed t-Test is a hypothesis test that is designed to show whether the mean of a sample is significantly greater than or significantly less than the mean of a population. If the resulting p-value of the two-tailed t-Test is greater than the selected alpha significance level, the null hypothesis is accepted. In this case the null hypothesis is that there is no difference in strength between the samples with and without sensors. The test was performed using Microsoft Excel's t-Test: Two-Sample Assuming Equal Variances with an alpha significance level of 0.05 for both the stress and strain t-tests. The resulting two-tailed p-value for stress is P(T<=t) 0.56, and P(T<=t) 0.88 for strain. It can be stated with confidence that the sensors can be seamlessly embedded into composites without impacting their structural integrity.

6.2 Impact of Resin Saturation on Sensor

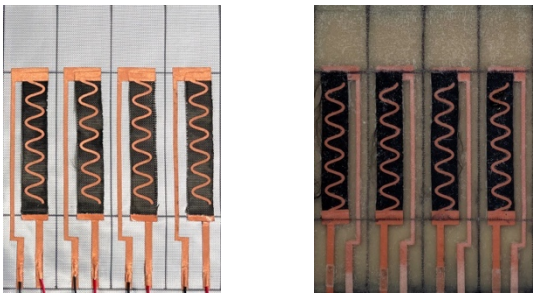

Figure 9: Sensors before (left) and after (right) being embedded in a composite and saturated with resin.

When the sensors are saturated with resin, their resistance increases dramatically and their performance changes. I took resistance readings from the sensors before and after being embedded in the composites to begin to characterize and understand these changes. Figure 9 shows images of the bend sensors described below, in Section 4.3, before and after embedment. Table 2 shows resistance measurements for these samples before and after saturation.

Table 2: Resistance reading before and after saturation – bending specimens.

Specimen	Resistance before saturation (kΩ)	Resistance after saturation (kΩ)	Percentage increase
1	1.26	2.29	82%
2	1.10	4.36	296%
3	0.73	2.13	192%
4	1.21	2.75	127%
5	0.73	4.78	555%

Average	1.01 (+/- 0.23)	3.26 (+/- 1.10)	224%

On average the resistance of sensors increased by 224% after being saturated with resin. However, a significant variation among the samples was observed. There are a few possible explanations for the changes in sensor resistance and the relatively high variability I observed. It is evident that the character of the polymerized fiberglass itself changes due to resin saturation. Changes in resistance that occur due to physical contact between fibers are decreased, since individual fibers are now coated in resin. On the other hand, changes that are intrinsic to the polymerized carbon coating the fibers become more dominant. It is also possible that the connections between the copper fabric and the polymerized fiberglass are impacted by this process.

6.3 Sensor Performance: Bending

To test the ability of the sensors to detect bending strain, we conducted a three-point bending test. In this test, shown in Figure 10. The test is performed by applying an intermediate load to a specimen spanning two supports. The load is applied in displacement control rate following ASTM D790 [8], with a span length of 100 mm. The specimen was oriented so that the sensor was at the bottom to observe tensile stresses, being stretched as the sample was bent. We constructed five samples for this test, an example of which is shown in Figure 10, right. These samples are all approximately 203mm long, 38mm wide, and 2.6mm thick.

We used the same Bionix universal testing machine that we employed in the structural integrity tests. We again used a controlled rate of displacement of 2 mm/minute. Force and strain data were collected through the FlexStar MTS® 793 data acquisition system with a sampling rate of 1 kHz. For this test, strain was recorded using linear pattern strain gauges from Omega Engineering [28]. These strain gages were attached to the bottom of each specimen at the midspan of the surface. The objective was to compare the strains measured by external strain gauges and that observed using the internal sensors.

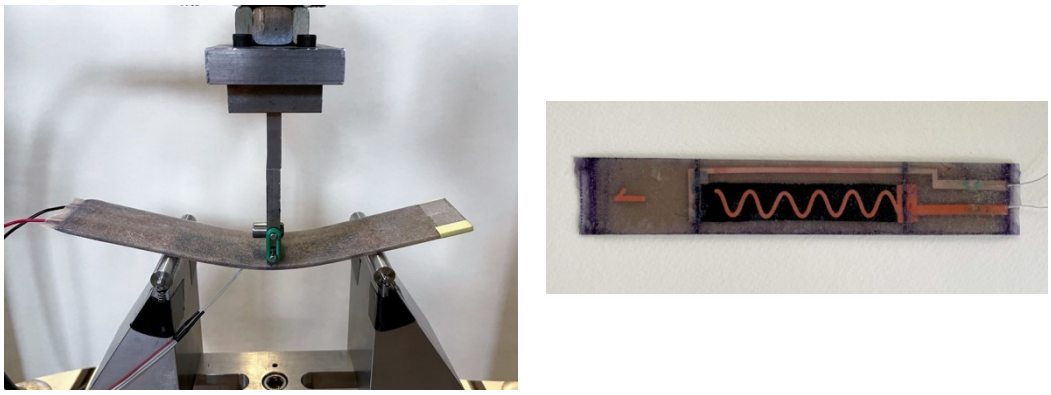

Figure 10: Left: The three-point bend test in progress. Right: one of the samples used for testing.

Figure 11 shows plots of the resistance values recorded from the sensors plotted versus strain measurements recorded from the external strain gauge. Figure 11, left shows the sensor data and Figure 11, right shows the percentage change in resistance versus strain. As can be observed in these graphs, for each individual sensor there seems to be an approximately linear relationship between the change in resistance, as measured by the sensors, and the change in strain. A linear

relationship between change in resistance and strain is desired because it enables the ability to estimate strain percentages from the resistance readings.

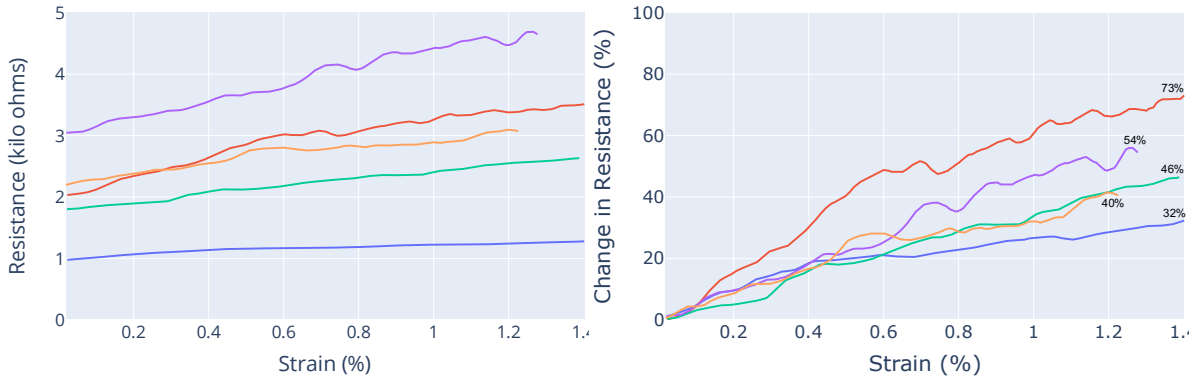

Figure 11: Three-point bend test, embedded sensor measurements. Left: Resistance vs. strain. Right: % change in resistance vs. strain.

These results are promising. However, there is noise present in the data for each sensor and variation in the slope of the curves between sensors. As can be seen in Figure 11, the percentage change in resistance experienced by the sensors ranged from 32% (at 1.40% strain) to 73% (at 1.40% strain), with the median sensor experiencing a 46% change (at 1.38% strain). Before the sensors can be used to predict strain reliably, I need to reduce this variability in performance. Section 7 details work to optimize the in-situ polymerization process to produce sensor material with reduced variability in performance.

6.4 Sensor Performance: Tension

During the structural integrity tests described in Section 4.1, data was recorded from the custom sensors as the samples were pulled apart. Figure 12

shows plots of these measurements for four of the five samples we created. The lines end at different points on the graph because the circuits broke, and I was no longer able to take resistance readings from the sensors. A testing error prevented us from obtaining data from the 5th sensor for this test.

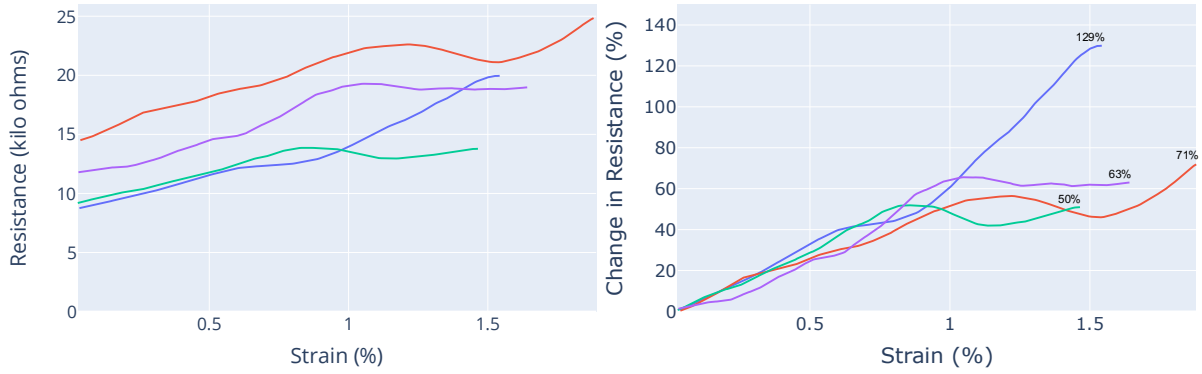

Figure 12: Tension test, embedded sensor measurements. Left: Resistance vs. strain. Right: % change in resistance vs. strain.

Again, for each sensor there seems to be an approximately linear relationship between the change in resistance measured by the sensors and the change in strain. However, I also see a significant variation between sensors here. It is interesting to note that the percentage change in resistance for these fours sensors diverges sharply at 1% strain, remaining relatively consistent before that threshold. This divergence may be attributed to the circuits beginning to break as the samples were being pulled apart, but further testing is needed to understand at what percent strain that the sensors fail.

7 DECREASING SENSOR VARIATION

After demonstrating the ability to seamlessly integrate sensors and circuits into structural composites, I needed to explore methods to decrease the variability of the sensors. To decrease variability between sensors, I revisited the in-situ polymerization process. I employed a technique described by Macasaquit et al. to find the optimal preparation conditions used to create piezoresistive fiberglass with a uniform resistance and coating [22]. Still using pyrrole as the monomer and iron chloride as the oxidizing agent, I varied the iron chloride concentration (7.5g, 10g, 15g, 20g), polymerization time (1 hr, 6 hr), agitation method (magnetic stirrer, flipping), and polymerization temperature (ice bath, no ice bath).

Based on the process described in Section 5.2, using a ratio of 1000:25 water to pyrrole—25ml of pyrrole for every 1 liter of water. I then used 7.5, 10, 15, or 20 grams of iron chloride for polymerization. The samples were left to polymerize for 1 or 6 hours while being agitated by either a magnetic stirrer or flipped every couple of minutes. The temperature during polymerization was varied by either placing the mixing container in an ice bath or not. Each sample was rinsed, and then scrubbed with a sponge remove any loose or excess polymers to create an even testing surface.

Samples of the different combinations were tested to compare resistance and functionality. 5 x 5 cm samples were cut from the polymerized sheets of fiberglass. I then measured the transverse resistance of the samples using the same process described in Section 5.2. A 10g weight was placed on the top electrode to ensure adequate electrode contact. The mean of one reading from each of the

samples, standard deviation, and coefficient of variation were calculated. The coefficient of variation, which is a ratio of the standard deviation to the mean, measures variability of data in a sample in relation to the mean. The results of this set of tests can be seen in Table 3.

Table 3: Transverse resistance and coefficient of variation for varying conditions for polymerization.

Conditions	Number of Samples	Mean Resting Resistance (kΩ)	Coefficient of Variation (%)
7.5g Iron Chloride 1 hr Polymerization Manual Agitation No Ice Bath	9	28.22 (+/- 9.97)	35.32%
10g Iron Chloride 1 hr Polymerization Manual Agitation No Ice Bath	9	7.44 (+/- 2.29)	30.73%
10g Iron Chloride 6 hr Polymerization Magnetic Stirrer Ice Bath	6	0.54 (+/- 0.15)	27.82%
15g Iron Chloride 6 hr Polymerization Magnetic Stirrer Ice Bath	6	4.91 (+/- 1.22)	24.77%
20g Iron Chloride 6 hr Polymerization Magnetic Stirrer Ice Bath	6	1.79 (+/-1.71)	95.79%

For comparison, I took transverse resistance readings from 10 samples that were not used for sensors embedded in composites. The mean and standard deviation of one reading from each of the samples was 109.09 (+/- 40.63833576) kΩ, with a coefficient of variation of 37.25%.

The samples created with 10g and 15g of iron chloride, polymerized for 6 hours, and mixed with the magnetic stirrer in an ice bath resulted in improved variability of 27.82% and 24.77% respectively. However, the sample made with 10g of iron chloride, polymerized for 6 hours, and mixed with the magnetic stirrer in an ice bath resulted has a much lower resistance of 0.54 kΩ compared to that of the other samples made during this exploration, and the sample made with 20g of iron chloride, polymerized for 6 hours, and mixed with the magnetic stirrer in an ice had a substantial variation of 95.79%.

Although I was able to reduce variability to 24.77%, it is still a significant amount of variation, and additional research needs to be done to further improve the polymerization process. As done by Macasaquit et al., a scanning electron microscope can be used to take images of the functional fiberglass to evaluate the binding of polymers to the surface of the fiberglass [22]. It would also be useful to continue to research methods for decreasing the variability of the polymerized fiberglass. For example, Krushnamurty et al. used a surfactant during the polymerization to help bind the piezoresistive polymers to the textile [19]. Next steps in this research would be to continue to evaluate methods to understand and decrease the variability of the functional fiberglass.

8 CONCLUSION

A new composite with a sensor and circuit fabricated from the composite's structural fabric was tested and validated. I determined that the proposed method of sensor and circuit construction does not affect the structural integrity of the composite. I demonstrated that the seamlessly integrated sensors can detect strain and constructed a proof-of-concept prototype that includes more complex circuitry and a microcontroller. In future work, the aim is to better understand sensor behavior during resin impregnation, continue to improve the reliability of sensor performance, and explore more complex applications that include embedded sensing, computation, and actuation. I believe that the ability to sense and respond to structural health information quickly and locally will open a range of exciting new possibilities in human infrastructure interaction.

9 REFERENCES

[1] Ahmed Al-Sabagh, Eman Taha, Usama Kandil, Ahmed Awadallah, Gamal-abdelnaser M. Nasr, and Mahmoud Reda Taha. 2017. Monitoring Moisture Damage Propagation in GFRP Composites Using Carbon Nanoparticles. *Polymers* 9, 3 (March 2017), 94. DOI:https://doi.org/10.3390/polym9030094

[2] Christos Andreades, Pooya Mahmoodi, and Francesco Ciampa. 2018. Characterisation of smart CFRP composites with embedded PZT transducers for nonlinear ultrasonic applications. *Composite Structures* 206, (December 2018), 456–466. DOI:https://doi.org/10.1016/j.compstruct.2018.08.083

[3] M. Boehle, Q. Jiang, L. Li, A. Lagounov, and K. Lafdi. 2012. Carbon nanotubes grown on glass fiber as a strain sensor for real time structural health monitoring. *International Journal of Smart and Nano Materials* 3, 2 (June 2012), 162–168. DOI:https://doi.org/10.1080/19475411.2011.651509

[4] Alberto Boem and Giovanni Maria Troiano. 2019. Non-Rigid HCI: A Review of Deformable Interfaces and Input. In *Proceedings of the 2019 on Designing Interactive Systems Conference*, ACM, San Diego CA USA, 885–906. DOI:https://doi.org/10.1145/3322276.3322347

[5] Leah Buechley and Michael Eisenberg. 2009. Fabric PCBs, electronic sequins, and socket buttons: techniques for e-textile craft. *Personal Ubiquitous Comput.* 13, 2 (2009), 133–150.

[6] Shaoluo Butler, Mark Gurvich, Anindya Ghoshal, Gregory Welsh, Paul Attridge, Howard Winston, Michael Urban, and Nathaniel Bordick. 2011. Effect of

embedded sensors on interlaminar damage in composite structures. *Journal of Intelligent Material Systems and Structures* 22, 16 (2011), 1857–1868. DOI:https://doi.org/10.1177/1045389X11414225

[7] Jian Cai, Lei Qiu, Shenfang Yuan, Lihua Shi, PeiPei Liu, and Dong Liang. 2012. *Structural Health Monitoring for Composite Materials*. IntechOpen. DOI:https://doi.org/10.5772/48215

[8] D20 Committee. *Test Methods for Flexural Properties of Unreinforced and Reinforced Plastics and Electrical Insulating Materials*. ASTM International. DOI:https://doi.org/10.1520/D0790-17

[9] Charles B. Duke. 1987. Metal-filled polymers—properties and applications, Swapan K. Bhattacharya, Ed., Marcel Dekker, New York, 1986, 360 pp. Price: $74.00. *Journal of Polymer Science: Polymer Letters Edition* 25, (1987), 263–263.

[10] Yu Enokibori and Kenji Mase. 2014. Human joint angle estimation with an e-textile sensor. In *Proceedings of the 2014 ACM International Symposium on Wearable Computers*, ACM, Seattle Washington, 129–130. DOI:https://doi.org/10.1145/2634317.2634331

[11] Fisher Scientific. Lab Equipment and Lab Supplies | Fisher Scientific. Retrieved September 9, 2021 from https://www.fishersci.com/us/en/home.html?cid=SEM_GAW_20190715_TFMZTQ&ppc_id=FisherSciBrand_goog_979894219_47449837174_fisher%20scientific_e_454244978520_14910766656890949204&s_kwcid=AL!4428!3!454244978520!e!!g!!__EFKW__&ef_id=Cj0KCQjw4eaJBhDMARIsANhrQADYBJG_IT3hjS

WidK76lH6_kXHN-gMZKlxXw-QDj5ap5rX_MLkzWrcaAnwnEALw_wcB:G:s&gclid=Cj0KCQjw4eaJBhDMARIsANhrQADYBJG_IT3hjSWidK76lH6_kXHN-gMZKlxXw-QDj5ap5rX_MLkzWrcaAnwnEALw_wcB

[12] Gerard J. Gallo and Erik T. Thostenson. 2015. Electrical characterization and modeling of carbon nanotube and carbon fiber self-sensing composites for enhanced sensing of microcracks. *Materials Today Communications* 3, (June 2015), 17–26. DOI:https://doi.org/10.1016/j.mtcomm.2015.01.009

[13] Oliver Glauser, Shihao Wu, Daniele Panozzo, Otmar Hilliges, and Olga Sorkine-Hornung. 2019. Interactive Hand Pose Estimation Using a Stretch-Sensing Soft Glove. *ACM Trans. Graph.* 38, 4 (July 2019). DOI:https://doi.org/10.1145/3306346.3322957

[14] Cedric Honnet, Hannah Perner-Wilson, Marc Teyssier, Bruno Fruchard, Jürgen Steimle, Ana C. Baptista, and Paul Strohmeier. 2020. PolySense: Augmenting Textiles with Electrical Functionality using In-Situ Polymerization. In *Proceedings of the 2020 CHI Conference on Human Factors in Computing Systems*, ACM, Honolulu HI USA, 1–13. DOI:https://doi.org/10.1145/3313831.3376841

[15] A. L. Kalamkarov, D. O. MacDonald, S. B. Fitzgerald, and A. V. Georgiades. 2000. Reliability assessment of pultruded FRP reinforcements with embedded fiber optic sensors. *Composite Structures* 50, 1 (September 2000), 69–78. DOI:https://doi.org/10.1016/S0263-8223(00)00081-7

[16] Konstantin Klamka, Raimund Dachselt, and Jürgen Steimle. 2020. Rapid Iron-On User Interfaces: Hands-on Fabrication of Interactive Textile Prototypes. In *Proceedings of the 2020 CHI Conference on Human Factors in Computing Systems*, ACM, Honolulu HI USA, 1–14. DOI:https://doi.org/10.1145/3313831.3376220

[17] Maris Knite, Valdis Teteris, Aleksandra Kiploka, and Jevgenijs Kaupuzs. 2004. Polyisoprene-carbon black nanocomposites as tensile strain and pressure sensor materials. *Sensors and Actuators A: Physical* 110, 1 (2004), 142–149. DOI:https://doi.org/10.1016/j.sna.2003.08.006

[18] Rebecca K. Kramer, Carmel Majidi, and Robert J. Wood. 2011. Wearable tactile keypad with stretchable artificial skin. In *2011 IEEE International Conference on Robotics and Automation*, 1103–1107. DOI:https://doi.org/10.1109/ICRA.2011.5980082

[19] K. Krushnamurty, M. Rini, I. Srikanth, P. Ghosal, A. P. Das, M. Deepa, and Ch Subrahmanyam. 2016. Conducting polymer coated graphene oxide reinforced C–epoxy composites for enhanced electrical conduction. *Composites Part A: Applied Science and Manufacturing* 80, (2016), 237–243. DOI:https://doi.org/10.1016/j.compositesa.2015.10.030

[20] Raghu Raja Pandiyan Kuppusamy, Satyajit Rout, and Kaushik Kumar. 2020. Chapter one - Advanced manufacturing techniques for composite structures used in aerospace industries. In *Modern Manufacturing Processes*, Kaushik Kumar and J. Paulo Davim (eds.). Woodhead Publishing, 3–12. DOI:https://doi.org/10.1016/B978-0-12-819496-6.00001-4

[21] LessEMF. 2007. Less EMF. Retrieved from http://www.lessemf.com/fabric.html/

[22] Anilyn C Macasaquit and Christina A Binag. 2010. Preparation of Conducting Polyester Textile by in situ Polymerization of Pyrrole. 139, 2 (2010), 8.

[23] Ye P. Mamunya, V. V. Davydenko, P. Pissis, and E. V. Lebedev. 2002. Electrical and thermal conductivity of polymers filled with metal powders. *European Polymer Journal* 38, 9 (2002), 1887–1897. DOI:https://doi.org/10.1016/S0014-3057(02)00064-2

[24] Stefano Mariani, Alberto Corigliano, Francesco Caimmi, Matteo Bruggi, Paolo Bendiscioli, and Marco De Fazio. 2013. MEMS-based surface mounted health monitoring system for composite laminates. *Microelectronics Journal* 44, 7 (July 2013), 598–605. DOI:https://doi.org/10.1016/j.mejo.2013.03.003

[25] Magdalena Mieloszyk, Katarzyna Majewska, and Wieslaw Ostachowicz. 2021. Application of embedded fibre Bragg grating sensors for structural health monitoring of complex composite structures for marine applications. *Marine Structures* 76, (2021), 102903. DOI:https://doi.org/10.1016/j.marstruc.2020.102903

[26] Magdalena Mieloszyk, Katarzyna Majewska, and Wieslaw Ostachowicz. 2021. Application of embedded fibre Bragg grating sensors for structural health monitoring of complex composite structures for marine applications. *Marine Structures* 76, (March 2021), 102903. DOI:https://doi.org/10.1016/j.marstruc.2020.102903

[27] Steven Nagels, Raf Ramakers, Kris Luyten, and Wim Deferme. 2018. Silicone Devices: A Scalable DIY Approach for Fabricating Self-Contained Multi-Layered Soft Circuits using Microfluidics. In *Proceedings of the 2018 CHI Conference on Human Factors in Computing Systems*, ACM, Montreal QC Canada, 1–13. DOI:https://doi.org/10.1145/3173574.3173762

[28] Omega Engineering. Omega Engineering | Shop for Sensing, Monitoring and Control Solutions with Technical Expertise. Retrieved September 7, 2021 from https://www.omega.com/en-us/?gclsrc=aw.ds&gclid=Cj0KCQjwm9yJBhDTARIsABKIcGbTLk_ys3wjMRUNUWImqEykY8PfqswoSBN41YakgV34BNeNFQjTzhQaAuGGEALw_wcB&gclsrc=aw.ds

[29] Plusea. Stickytape Sensors. *Instructables*. Retrieved October 31, 2021 from https://www.instructables.com/Stickytape-Sensors/

[30] Stefan Schneegass, Kristof Van Laerhoven, Jingyuan Cheng, and Oliver Amft. 2014. Workshop on smart garments: sensing, actuation, interaction, and applications in garments. In *Proceedings of the 2014 ACM International Symposium on Wearable Computers Adjunct Program - ISWC '14 Adjunct*, ACM Press, Seattle, Washington, 225–229. DOI:https://doi.org/10.1145/2641248.2666712

[31] J. Sebastian, N. Schehl, M. Bouchard, M. Boehle, L. Li, A. Lagounov, and K. Lafdi. 2014. Health monitoring of structural composites with embedded carbon nanotube coated glass fiber sensors. *Carbon* 66, (January 2014), 191–200. DOI:https://doi.org/10.1016/j.carbon.2013.08.058

[32] Anjali Singhvi, Mike Baker, Weiyi Cai, Mika Gröndahl, and Karthik Patanjali. 2021. The Surfside Condo Was Flawed and Failing. Here's a Look Inside. *The New York Times*. Retrieved September 9, 2021 from https://www.nytimes.com/interactive/2021/09/01/us/miami-building-collapse.html

[33] Ronit Slyper, Ivan Poupyrev, and Jessica Hodgins. 2010. Sensing through structure: designing soft silicone sensors. In *Proceedings of the fifth international conference on Tangible, embedded, and embodied interaction*, ACM, Funchal Portugal, 213–220. DOI:https://doi.org/10.1145/1935701.1935744

[34] Hong-Yue Tang, Charles Winkelmann, Wahyu Lestari, and Valeria La Saponara. 2011. Composite Structural Health Monitoring Through Use of Embedded PZT Sensors. *Journal of Intelligent Material Systems and Structures* 22, 8 (May 2011), 739–755. DOI:https://doi.org/10.1177/1045389X11406303

[35] US Composites. Fiberglass , Epoxy , Composites, Carbon Fiber - U.S. Composites, Inc. Retrieved September 7, 2021 from http://www.uscomposites.com/

[36] Shoukai Wang, Daniel P. Kowalik, and D. D. L. Chung. 2004. Self-sensing attained in carbon-fiber–polymer-matrix structural composites by using the interlaminar interface as a sensor. *Smart Mater. Struct.* 13, 3 (May 2004), 570–592. DOI:https://doi.org/10.1088/0964-1726/13/3/017

[37] Xue Yan, Charles RP Courtney, Chris R Bowen, Nicholas Gathercole, Tao Wen, Yu Jia, and Yu Shi. 2020. In situ fabrication of carbon fibre–reinforced polymer

composites with embedded piezoelectrics for inspection and energy harvesting applications. *Journal of Intelligent Material Systems and Structures* 31, 16 (September 2020), 1910–1919. DOI:https://doi.org/10.1177/1045389X20942315

[38] Yang Yang, Thomas Vervust, Sheila Dunphy, Steven Van Put, Bjorn Vandecasteele, Kristof Dhaenens, Lieven Degrendele, Lothar Mader, Linde De Vriese, Tom Martens, Markus Kaufmann, Tsuyoshi Sekitani, and Jan Vanfleteren. 2018. 3D Multifunctional Composites Based on Large-Area Stretchable Circuit with Thermoforming Technology. *Advanced Electronic Materials* 4, 8 (2018), 1800071. DOI:https://doi.org/10.1002/aelm.201800071